Two-qubit and three-qubit controlled gates with cross-Kerr nonlinearity*

Zhao Rui-Tong(赵瑞通)[a], Guo Qi(郭 奇)[b], Cheng Liu-Yong(程留永)[b], Sun Li-Li(孙立莉)[b], Wang Hong-Fu(王洪福)[a], and Zhang Shou(张 寿)[a]†

[a] *Department of Physics, College of Science, Yanbian University, Yanji* 133002, *China*

[b] *Center for the Condensed-Matter Science and Technology, Department of Physics, Harbin Institute of Technology, Harbin* 150001, *China*

(Received 30 July 2012; revised manuscript received 10 September 2012)

Schemes for two-qubit and three-qubit controlled gates based on cross-Kerr nonlinearity are proposed in this paper. The probability of the success of these gates can be increased by quantum nondemolition detectors, which are used to judge which paths the signal photons pass through. These schemes are almost deterministic and require no ancilla photon. The advantages of these gates over the existing ones include less resource consumption and a higher probability of success, which make our schemes more feasible with current technology.

Keywords: quantum controlled gates, cross-Kerr nonlinearity, quantum nondemolition detector

PACS: 03.67.–a, 03.67.Lx, 42.50.Ex **DOI:** 10.1088/1674-1056/22/3/030313

1. Introduction

Due to their power, which is much more efficient and faster than in classical computers, quantum computers have attracted much attention in the last few years. Quantum controlled gates play a very important role in quantum computation. Many physical systems have been considered to implement quantum controlled gates,[1–4] and a promising one is the optical system, which has advantages such as low decoherence and easy single-qubit manipulation. However, because of the lack of interaction between individual photon qubits, such a system suffers the major disadvantage of implementing multi-qubit controlled gates. Fortunately, Knill, Laflamme, and Milburn showed that two-qubit quantum gates such as controlled-NOT (CNOT) gates can be implemented with a certain probability using auxiliary single photons, linear optical elements, single photon detectors, and feedforward.[5] Since then, many schemes have been proposed for linear optical quantum controlled gates.[6–12] Pittman *et al.* showed how to implement a CNOT gate using polarizing beam splitters (PBS).[6] Hofmann *et al.* showed that a quantum phase gate operation can be realized with beam splitters (BS) if only the outputs are postselected.[9] However, all these gates are probabilistic, which makes the realization of multi-qubit controlled gates and universal quantum computation impractical. For example, the quantum Fredkin gate proposed in Ref. [13] can be realized with a probability of $4^{-5} \approx 1.0 \times 10^{-3}$, in which the probability of the CNOT gate used in the Fredkin gate is $1/4$.[6]

To avoid this inefficiency, more efficient quantum controlled gates with weak cross-Kerr nonlinearity have been proposed.[14,15] Nemoto *et al.* presented an almost deterministic optical CNOT gate using several single photons, linear optical elements, and photon number resolving quantum nondemolition detectors based on weak cross-Kerr nonlinearity and feedforward.[15] Some people have witnessed great progress in the development of single-photon quantum computing and quantum information processing. Many schemes for devising two-qubit gates via weak cross-Kerr nonlinearity have been presented.[16–19] However, universal computation, even a multi-qubit gate, may need many CNOT gates, which makes the structure too complex to be realized in practice. Thus, it is necessary to study the direct realization of multi-qubit gates with simpler structures. In 2009, Lin *et al.* showed the realization of quantum control gates, including the CNOT gate, Fredkin gate, Toffoli gate, arbitrary controlled-U gate, and even arbitrary multi-controlled-U gate.[20] Only the coherent states and no ancilla photon are required, and all these gates are scalable with certain probabilities larger than those gates in linear optics, but not deterministic. Motivated by the scheme of Lin *et al.*, we present new schemes for implementing two-qubit and three-qubit optical controlled gates with cross-Kerr nonlinearities and basic optical elements.

This paper is organized as follows. In Section 2, we discuss our schemes for two-qubit controlled gates, which are based on weak cross-Kerr nonlinearities, in detail. In the present scheme, no ancilla photon is required, which reduces resource consumption. Furthermore, we utilize quantum nondemolition (QND) detectors, by which we can detect the existence of photons without destroying them, so that the success

*Project supported by the National Natural Science Foundation of China (Grant Nos. 61068001 and 11264042) and the Program for Chun Miao Excellent Talents of Department of Education of Jilin Province, China (Grant No. 201316).

†Corresponding author. E-mail: szhang@ybu.edu.cn

© 2013 Chinese Physical Society and IOP Publishing Ltd

probability of the gates is increased. Through classical feedforwards according to the outcomes of QND detectors, our protocol can be implemented with an almost deterministic success probability. Moreover, this technique is developed to realize the three-qubit controlled gates in Section 3. All of these gates are almost deterministic and require no ancilla photon. Finally, Section 4 presents the discussion and conclusion.

2. Two-qubit controlled gates with cross-Kerr nonlinearity

Before expounding our schemes for the controlled gates, we first introduce the cross-Kerr nonlinearity. The cross-Kerr nonlinearity has a Hamiltonian in the following form:[21]

$$H = \hbar\chi a_{\rm s}^{\dagger}a_{\rm s}a_{\rm p}^{\dagger}a_{\rm p}. \tag{1}$$

Here $a_{\rm s}^{\dagger}(a_{\rm p}^{\dagger})$ and $a_{\rm s}(a_{\rm p})$ represent the creation and annihilation operations, respectively, and the subscript s (p) denotes the signal (probe) mode. χ is the coupling strength of the nonlinearity, which is decided by the property of the cross-Kerr medium. Suppose that the signal field is in state $|n_{\rm a}\rangle$ and the probe beam is the coherent state $|\alpha\rangle$. After photons pass through the cross-Kerr medium, the joint state of the combined system will be

$$|\Psi\rangle = {\rm e}^{{\rm i}\chi t a_{\rm s}^{\dagger}a_{\rm s}a_{\rm p}^{\dagger}a_{\rm p}}|n_{\rm a}\rangle|\alpha\rangle = |n_{\rm a}\rangle|\alpha\,{\rm e}^{{\rm i}n_{\rm a}\theta}\rangle, \tag{2}$$

where $\theta = \chi t$ and t is the interaction time. Thus, by the measurement on the phase of the probe beam, we can distinguish the photon numbers in the signal mode, that is, the state $|\Psi\rangle$ will project into a number state.

Now, we discuss the two-qubit controlled-Z gate. Suppose that two photons are initially prepared in the state

$$\begin{aligned}|\Psi\rangle_{\rm in} &= \alpha|H\rangle_{\rm c}|H\rangle_{\rm t} + \beta|H\rangle_{\rm c}|V\rangle_{\rm t}\\ &\quad + \gamma|V\rangle_{\rm c}|H\rangle_{\rm t} + \delta|V\rangle_{\rm c}|V\rangle_{\rm t}.\end{aligned} \tag{3}$$

The setup of the two-qubit controlled-Z gate is shown in Fig. 1. The control photon and target photon pass through $\rm PBS_1$ and $\rm PBS_2$, respectively. Then, the states in spatial modes $\rm t_1$ and $\rm t_2$ mix at a 50:50 BS. The action of the BS can be described by the transformation

$$a_{\rm t_1}^{\dagger} \to \frac{1}{\sqrt{2}}(a_{\rm t_1}^{\dagger} + a_{\rm t_2}^{\dagger}), \tag{4}$$

$$a_{\rm t_2}^{\dagger} \to \frac{1}{\sqrt{2}}(a_{\rm t_1}^{\dagger} - a_{\rm t_2}^{\dagger}). \tag{5}$$

Thus, the state of the photons will be

$$\begin{aligned}|\Psi\rangle_{\rm in} &= \frac{1}{\sqrt{2}}(\alpha|H\rangle_{\rm c_1}|H\rangle_{\rm t_1} + \beta|H\rangle_{\rm c_1}|V\rangle_{\rm t_1}\\ &\quad + \gamma|V\rangle_{\rm c_2}|H\rangle_{\rm t_2} - \delta|V\rangle_{\rm c_2}|V\rangle_{\rm t_2}\\ &\quad + \alpha|H\rangle_{\rm c_1}|H\rangle_{\rm t_2} - \beta|H\rangle_{\rm c_1}|V\rangle_{\rm t_2}\\ &\quad + \gamma|V\rangle_{\rm c_2}|H\rangle_{\rm t_1} + \delta|V\rangle_{\rm c_2}|V\rangle_{\rm t_1}).\end{aligned} \tag{6}$$

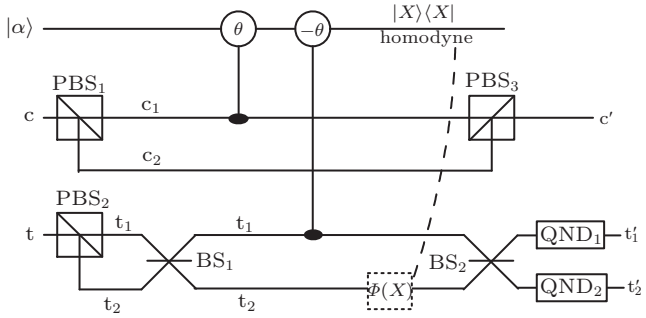


Fig. 1. The two-qubit controlled-Z gate. BS and PBS denote the beam splitter and polarizing beam splitter, respectively, $\Phi(X)$ denotes a phase shift dependent on the feedforward result of the homodyne measurement, and QND denotes the quantum nondemolition detector.

After the cross-Kerr nonlinearity interaction, the evolution of the joint state of the combined system is given by

$$\begin{aligned}&|\Psi\rangle_{\rm in}|\alpha\rangle \to |\Psi\rangle\\ &= \frac{1}{\sqrt{2}}[(\alpha|H\rangle_{\rm c_1}|H\rangle_{\rm t_1} + \beta|H\rangle_{\rm c_1}|V\rangle_{\rm t_1}\\ &\quad + \gamma|V\rangle_{\rm c_2}|H\rangle_{\rm t_2} - \delta|V\rangle_{\rm c_2}|V\rangle_{\rm t_2})|\alpha\rangle\\ &\quad + (\alpha|H\rangle_{\rm c_1}|H\rangle_{\rm t_2} - \beta|H\rangle_{\rm c_1}|V\rangle_{\rm t_2})|\alpha\,{\rm e}^{{\rm i}\theta}\rangle\\ &\quad + (\gamma|V\rangle_{\rm c_2}|H\rangle_{\rm t_1} + \delta|V\rangle_{\rm c_2}|V\rangle_{\rm t_1})|\alpha\,{\rm e}^{-{\rm i}\theta}\rangle].\end{aligned} \tag{7}$$

Afterwards, an X homodyne measurement,[15] with which the $|\alpha\,{\rm e}^{{\rm i}\theta}\rangle$ and $|\alpha\,{\rm e}^{-{\rm i}\theta}\rangle$ states cannot be distinguished, is performed on the coherent beam. With real α, an X homodyne measurement projects $|\Psi\rangle$ onto the eigenstate $|X\rangle$ of the observable X. The resulting two photonic states are

$$\begin{aligned}|\Psi\rangle_X &= \langle X|\Psi\rangle\\ &= \frac{1}{\sqrt{2}}\{f(X,\alpha)(\alpha|H\rangle_{\rm c_1}|H\rangle_{\rm t_1} + \beta|H\rangle_{\rm c_1}|V\rangle_{\rm t_1}\\ &\quad + \gamma|V\rangle_{\rm c_2}|H\rangle_{\rm t_2} - \delta|V\rangle_{\rm c_2}|V\rangle_{\rm t_2})\\ &\quad + f(X,\alpha\cos\theta)[{\rm e}^{{\rm i}\Phi(X)}(\alpha|H\rangle_{\rm c_1}|H\rangle_{\rm t_2} - \beta|H\rangle_{\rm c_1}|V\rangle_{\rm t_2})\\ &\quad + {\rm e}^{-{\rm i}\Phi(X)}(\gamma|V\rangle_{\rm c_2}|H\rangle_{\rm t_1} + \delta|V\rangle_{\rm c_2}|V\rangle_{\rm t_1})]\},\end{aligned} \tag{8}$$

where

$$\begin{aligned}f(X,\varepsilon) &= \frac{1}{\sqrt[4]{2\pi}}\exp\left[-\frac{1}{4}(x-2\varepsilon)^2\right],\\ \Phi(X) &= \alpha\sin\theta(x - 2\alpha\cos\theta){\rm mod}(2\pi).\end{aligned}$$

We see that $f(X,\alpha)$ and $f(X,\alpha\cos\theta)$ are two Gaussian curves, with the midpoint between the peaks located at $X_0 = \alpha(1+\cos\theta)$ and the peaks separated by a distance $X_{\rm d} = 2\alpha(1-\cos\theta)$. As long as this difference is large ($X_{\rm d} \sim \alpha\theta^2 \gg 1$), there is little overlap between these curves. For $X > X_0$, we have

$$\begin{aligned}|\Psi\rangle_{X>X_0} &\sim \alpha|H\rangle_{\rm c_1}|H\rangle_{\rm t_1} + \beta|H\rangle_{\rm c_1}|V\rangle_{\rm t_1}\\ &\quad + \gamma|V\rangle_{\rm c_2}|H\rangle_{\rm t_2} - \delta|V\rangle_{\rm c_2}|V\rangle_{\rm t_2}.\end{aligned} \tag{9}$$

Due to PBS_3 and BS_2, this state will become

$$\begin{aligned}|\Psi\rangle_{\rm out} = & \frac{1}{\sqrt{2}}(\alpha|H\rangle_{c'}|H\rangle_{t'_1}+\beta|H\rangle_{c'}|V\rangle_{t'_1}\\ & +\gamma|V\rangle_{c'}|H\rangle_{t'_1}-\delta|V\rangle_{c'}|V\rangle_{t'_1}\\ & +\alpha|H\rangle_{c'}|H\rangle_{t'_2}+\beta|H\rangle_{c'}|V\rangle_{t'_2}\\ & -\gamma|V\rangle_{c'}|H\rangle_{t'_2}+\delta|V\rangle_{c'}|V\rangle_{t'_2}). \end{aligned} \tag{10}$$

If the target photon passes through path t'_1, then the state of the photons will be $|\Psi\rangle_1 = \alpha|H\rangle_{c'}|H\rangle_{t'_1}+\beta|H\rangle_{c'}|V\rangle_{t'_1}+\gamma|V\rangle_{c'}|H\rangle_{t'_1}-\delta|V\rangle_{c'}|V\rangle_{t'_1}$. It is immediately apparent that the two-qubit controlled-Z operation is completed. Otherwise, the photons will be in state $|\Psi\rangle_2 = \alpha|H\rangle_{c'}|H\rangle_{t'_1}+\beta|H\rangle_{c'}|V\rangle_{t'_1}-\gamma|V\rangle_{c'}|H\rangle_{t'_1}+\delta|V\rangle_{c'}|V\rangle_{t'_1}$, which can be converted into $|\Psi\rangle_1$ by a σ_z operation on path c'.

For $X < X_0$, the two photons will be in state

$$\begin{aligned}|\Psi\rangle_{X<X_0} = & \ {\rm e}^{{\rm i}\Phi(X)}(\alpha|H\rangle_{c_1}|H\rangle_{t_2}-\beta|H\rangle_{c_1}|V\rangle_{t_2})\\ & +{\rm e}^{-{\rm i}\Phi(X)}(\gamma|V\rangle_{c_2}|H\rangle_{t_1}+\delta|V\rangle_{c_2}|V\rangle_{t_1}). \end{aligned} \tag{11}$$

Then, a phase shift should be performed on path t_2 to achieve the state

$$\begin{aligned}|\Psi\rangle'_{X<X_0} = & \ \alpha|H\rangle_{c_1}|H\rangle_{t_2}-\beta|H\rangle_{c_1}|V\rangle_{t_2}\\ & +\gamma|V\rangle_{c_2}|H\rangle_{t_1}+\delta|V\rangle_{c_2}|V\rangle_{t_1}. \end{aligned} \tag{12}$$

As a result of PBS_3 and BS_2, the photons will be in state

$$\begin{aligned}|\Psi\rangle'_{\rm out} = & \frac{1}{\sqrt{2}}(\alpha|H\rangle_{c'}|H\rangle_{t'_1}-\beta|H\rangle_{c'}|V\rangle_{t'_1}\\ & +\gamma|V\rangle_{c'}|H\rangle_{t'_1}+\delta|V\rangle_{c'}|V\rangle_{t'_1}\\ & -\alpha|H\rangle_{c'}|H\rangle_{t'_2}+\beta|H\rangle_{c'}|V\rangle_{t'_2}\\ & +\gamma|V\rangle_{c'}|H\rangle_{t'_2}+\delta|V\rangle_{c'}|V\rangle_{t'_2}). \end{aligned} \tag{13}$$

Similar to the case of no phase shift, the controlled-Z operation can be implemented by σ_z operations on corresponding paths according to the outcomes of the QND detectors through a classical feedforward. A σ_z operation will be performed on path t'_1, if the target photon passes through path t'_1. When the photon passes through path t'_2, the σ_z operations will be performed on paths c' and t'_2.

It is worth noting that there is a small but finite probability that the state given by Eq. (9) can occur for $X < X_0$, and vice versa. The small overlap between the two Gaussian curves amounts to the error probability,[14] which is given by

$$P_{\rm error} = \frac{1}{2}{\rm erfc}[X_{\rm d}/2\sqrt{2}].$$

The $P_{\rm error}$ is less than 10^{-5} when $X_{\rm d} \sim \alpha\theta^2 > 9$. Thus, this controlled-Z gate is nearly deterministic, and a CNOT gate can be constructed utilizing this controlled-Z gate and two half-wave plants (HWPs), which implement Hadamard operations on the target photon. The CNOT gate proposed in Ref. [15] is almost deterministic. However, this scheme needs two parity detectors based on cross-Kerr nonlinearity, and also one ancilla photon, which makes the structure complex. Lin *et al.*[20] simplified the structure of the CNOT gate, which needs only one parity detector and no ancilla photon, at the cost of reducing the probability of success. Because of the QND detectors, our scheme is almost deterministic and consumes less resources due to no auxiliary photons.

The two-qubit controlled gates can be generalized to the nonlocal field directly. Suppose that two parties, Alice and Bob, located in different places, share the two-qubit state given by Eq. (3) with each qubit at a different spatial location. After the interaction between the control photon and the probe beam, with the help of cross-Kerr nonlinearity, the probe beam is transmitted to Bob, who also used cross-Kerr nonlinearity to make the target photon interact with the probe field. The nonlocal two-qubit controlled gates can be implemented by appropriate operations performed by Bob according to the homodyne measurement and the outcomes of QND detectors through classical feedforwards.

3. Three-qubit controlled gates with cross-Kerr nonlinearity

In this section, we discuss three-qubit controlled gates with cross-Kerr nonlinearity. Two common three-qubit controlled gates are the Fredkin gate and Toffoli gate. First, we pay attention to the implementation of the Fredkin gate. The schematic structure of our Fredkin gate is shown in Fig. 2. Compared with the two-qubit gate, we change the phase shift induced by the control photon to be 3θ, while the phase shift is -2θ and $-\theta$ for the two target photons, respectively. To show how the scheme works, we consider an arbitrary input state

$$\begin{aligned}|\Psi\rangle_{\rm in} = & \ a_1|H\rangle_{c}|H\rangle_{t_1}|H\rangle_{t_2}+a_2|H\rangle_{c}|H\rangle_{t_1}|V\rangle_{t_2}\\ & +a_3|H\rangle_{c}|V\rangle_{t_1}|H\rangle_{t_2}+a_4|H\rangle_{c}|V\rangle_{t_1}|V\rangle_{t_2}\\ & +a_5|V\rangle_{c}|H\rangle_{t_1}|H\rangle_{t_2}+a_6|V\rangle_{c}|H\rangle_{t_1}|V\rangle_{t_2}\\ & +a_7|V\rangle_{c}|V\rangle_{t_1}|H\rangle_{t_2}+a_8|V\rangle_{c}|V\rangle_{t_1}|V\rangle_{t_2}. \end{aligned} \tag{14}$$

The control photon is transmitted through PBS_1, while the two target photons are transmitted through BS_1 and BS_2, respectively. After the cross-Kerr nonlinearity interaction, the evolution of the system state is governed by

$$\begin{aligned}& |\Psi\rangle_{\rm in}|\alpha\rangle \to |\Psi\rangle\\ = & \frac{1}{2}[(a_1|H\rangle_1|H\rangle_3|H\rangle_5+a_2|H\rangle_1|H\rangle_3|V\rangle_5\\ & +a_3|H\rangle_1|V\rangle_3|H\rangle_5+a_4|H\rangle_1|V\rangle_3|V\rangle_5\\ & +a_5|V\rangle_2|H\rangle_4|H\rangle_6+a_6|V\rangle_2|H\rangle_4|V\rangle_6\\ & +a_7|V\rangle_2|V\rangle_4|H\rangle_6+a_8|V\rangle_2|V\rangle_4|V\rangle_6)|\alpha\rangle\\ & +(a_1|H\rangle_1|H\rangle_3|H\rangle_6+a_2|H\rangle_1|H\rangle_3|V\rangle_6 \end{aligned}$$

$$
\begin{aligned}
&+a_3|H\rangle_1|V\rangle_3|H\rangle_6+a_4|H\rangle_1|V\rangle_3|V\rangle_6)|\alpha\mathrm{e}^{\mathrm{i}\theta}\rangle\\
&+(a_5|V\rangle_2|H\rangle_4|H\rangle_5+a_6|V\rangle_2|H\rangle_4|V\rangle_5\\
&+a_7|V\rangle_2|V\rangle_4|H\rangle_5+a_8|V\rangle_2|V\rangle_4|V\rangle_5)|\alpha\mathrm{e}^{-\mathrm{i}\theta}\rangle\\
&+(a_1|H\rangle_1|H\rangle_4|H\rangle_5+a_2|H\rangle_1|H\rangle_4|V\rangle_5\\
&+a_3|H\rangle_1|V\rangle_4|H\rangle_5+a_4|H\rangle_1|V\rangle_4|V\rangle_5)|\alpha\mathrm{e}^{\mathrm{i}2\theta}\rangle\\
&+(a_5|V\rangle_2|H\rangle_3|H\rangle_6+a_6|V\rangle_2|H\rangle_3|V\rangle_6\\
&+a_7|V\rangle_2|V\rangle_3|H\rangle_6+a_8|V\rangle_2|V\rangle_3|V\rangle_6)|\alpha\mathrm{e}^{-\mathrm{i}2\theta}\rangle\\
&+(a_1|H\rangle_1|H\rangle_4|H\rangle_6+a_2|H\rangle_1|H\rangle_4|V\rangle_6\\
&+a_3|H\rangle_1|V\rangle_4|H\rangle_6+a_4|H\rangle_1|V\rangle_4|V\rangle_6)|\alpha\mathrm{e}^{\mathrm{i}3\theta}\rangle\\
&+(a_5|V\rangle_2|H\rangle_3|H\rangle_5+a_6|V\rangle_2|H\rangle_3|V\rangle_5\\
&+a_7|V\rangle_2|V\rangle_3|H\rangle_5+a_8|V\rangle_2|V\rangle_3|V\rangle_5)|\alpha\mathrm{e}^{-\mathrm{i}3\theta}\rangle]. \quad (15)
\end{aligned}
$$

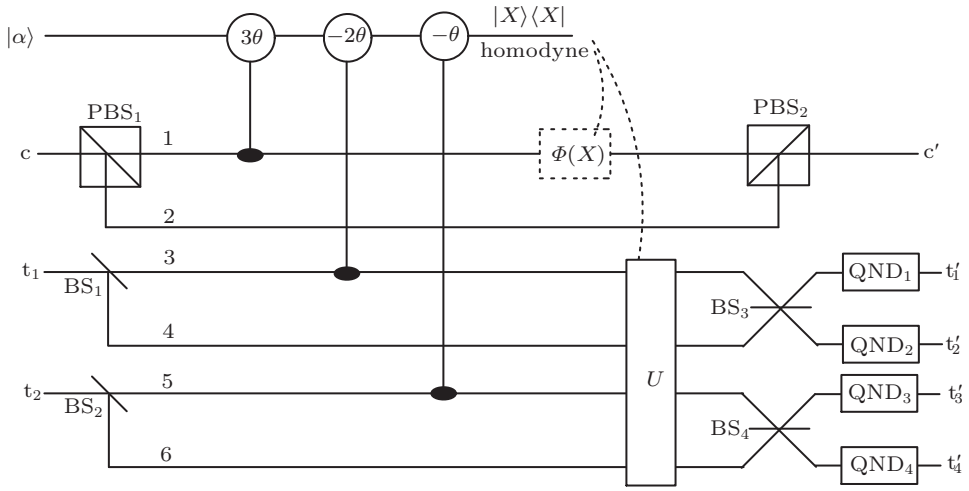


Fig. 2. The three-qubit Fredkin gate. U denotes operation in the target photons and $\Phi(X)$ represents a phase shift, both of which are controlled by the homodyne measurement on the coherent beam through a classical feedforward.

After X homodyne measurement on the coherent beam, the state will be

$$
\begin{aligned}
|\Psi\rangle_X &= \langle X|\Psi\rangle\\
&= \frac{1}{2}\{f(X,\alpha)(a_1|H\rangle_1|H\rangle_3|H\rangle_5+a_2|H\rangle_1|H\rangle_3|V\rangle_5\\
&\quad+a_3|H\rangle_1|V\rangle_3|H\rangle_5+a_4|H\rangle_1|V\rangle_3|V\rangle_5\\
&\quad+a_5|V\rangle_2|H\rangle_4|H\rangle_6+a_6|V\rangle_2|H\rangle_4|V\rangle_6\\
&\quad+a_7|V\rangle_2|V\rangle_4|H\rangle_6+a_8|V\rangle_2|V\rangle_4|V\rangle_6)\\
&\quad+f(X,\alpha\cos\theta)[\mathrm{e}^{\mathrm{i}\Phi(X)_1}(a_1|H\rangle_1|H\rangle_3|H\rangle_6\\
&\quad+a_2|H\rangle_1|H\rangle_3|V\rangle_6+a_3|H\rangle_1|V\rangle_3|H\rangle_6\\
&\quad+a_4|H\rangle_1|V\rangle_3|V\rangle_6)\\
&\quad+\mathrm{e}^{-\mathrm{i}\Phi(X)_1}(a_5|V\rangle_2|H\rangle_4|H\rangle_5+a_6|V\rangle_2|H\rangle_4|V\rangle_5\\
&\quad+a_7|V\rangle_2|V\rangle_4|H\rangle_5+a_8|V\rangle_2|V\rangle_4|V\rangle_5)]\\
&\quad+f(X,\alpha\cos2\theta)[\mathrm{e}^{\mathrm{i}\Phi(X)_2}(a_1|H\rangle_1|H\rangle_4|H\rangle_5\\
&\quad+a_2|H\rangle_1|H\rangle_4|V\rangle_5+a_3|H\rangle_1|V\rangle_4|H\rangle_5\\
&\quad+a_|H\rangle_1|V\rangle_4|V\rangle_5)\\
&\quad+\mathrm{e}^{-\mathrm{i}\Phi(X)_2}(a_5|V\rangle_2|H\rangle_3|H\rangle_6+a_6|V\rangle_2|H\rangle_3|V\rangle_6\\
&\quad+a_7|V\rangle_2|V\rangle_3|H\rangle_6+a_8|V\rangle_2|V\rangle_3|V\rangle_6)]\\
&\quad+f(X,\alpha\cos3\theta)[\mathrm{e}^{\mathrm{i}\Phi(X)_3}(a_1|H\rangle_1|H\rangle_4|H\rangle_6\\
&\quad+a_2|H\rangle_1|H\rangle_4|V\rangle_6+a_3|H\rangle_1|V\rangle_4|H\rangle_6\\
&\quad+a_4|H\rangle_1|V\rangle_4|V\rangle_6)\\
&\quad+\mathrm{e}^{-\mathrm{i}\Phi(X)_3}(a_5|V\rangle_2|H\rangle_3|H\rangle_5+a_6|V\rangle_2|H\rangle_3|V\rangle_5\\
&\quad+a_7|V\rangle_2|V\rangle_3|H\rangle_5+a_8|V\rangle_2|V\rangle_3|V\rangle_5)]\}, \quad (16)
\end{aligned}
$$

where $\Phi(X)_j = \alpha\sin(j\theta)[x-2\alpha\cos(j\theta)]\mathrm{mod}(2\pi)$ $(j=1,2,3)$. We observe that $f(X,\varepsilon)$ are four Gaussian curves with the peaks located at $2\alpha\cos(n\theta)$ $(n=0,1,2,3)$, respectively. The neighboring peaks are separated by the distances $X_{\mathrm{d}_j} = 2\alpha\{\cos[(j-1)\theta]-\cos(j\theta)\}$. When $\theta \ll 1$, $X_{\mathrm{d}_j} \sim (2j-1)\alpha\theta^2$. Near the peak of $f(X,\alpha)$, no phase shift is induced in the coherent state, and thus the three photons will be projected into the state

$$
\begin{aligned}
|\Psi\rangle_1 &= a_1|H\rangle_1|H\rangle_3|H\rangle_5+a_2|H\rangle_1|H\rangle_3|V\rangle_5\\
&\quad+a_3|H\rangle_1|V\rangle_3|H\rangle_5+a_4|H\rangle_1|V\rangle_3|V\rangle_5\\
&\quad+a_5|V\rangle_2|H\rangle_4|H\rangle_6+a_6|V\rangle_2|H\rangle_4|V\rangle_6\\
&\quad+a_7|V\rangle_2|V\rangle_4|H\rangle_6+a_8|V\rangle_2|V\rangle_4|V\rangle_6. \quad (17)
\end{aligned}
$$

After that a U operation is performed on the two target photons, which implement the swap operation on the state in spatial modes 4 and 6, that is, the transformations $\{|HH\rangle_{46}\rightarrow|HH\rangle_{46}, |HV\rangle_{46}\rightarrow|VH\rangle_{46}, |VH\rangle_{46}\rightarrow|HV\rangle_{46}, |VV\rangle_{46}\rightarrow|VV\rangle_{46}\}$ will be completed. The swap operation on two spatial modes can be achieved by the setup shown in Fig. 3. Due to the effect of the U operation, the state $|\Psi\rangle_1$ will be converted into

$$
\begin{aligned}
|\Psi\rangle_1' &= a_1|H\rangle_1|H\rangle_3|H\rangle_5+a_2|H\rangle_1|H\rangle_3|V\rangle_5\\
&\quad+a_3|H\rangle_1|V\rangle_3|H\rangle_5+a_4|H\rangle_1|V\rangle_3|V\rangle_5\\
&\quad+a_5|V\rangle_2|H\rangle_4|H\rangle_6+a_6|V\rangle_2|V\rangle_4|H\rangle_6\\
&\quad+a_7|V\rangle_2|H\rangle_4|V\rangle_6+a_8|V\rangle_2|V\rangle_4|V\rangle_6. \quad (18)
\end{aligned}
$$

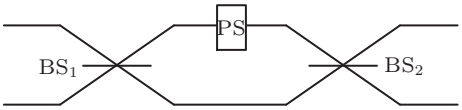


Fig. 3. The swap operation on two spatial modes. PS denotes a phase shift of π in the upper arm.

After passing through PBS_2, BS_3, and BS_4, the state will be converted into

$$\begin{aligned}|\Psi\rangle_1' \rightarrow \frac{1}{2}[&a_1|H\rangle_{c'}|H\rangle_{t_1'}|H\rangle_{t_3'}+a_2|H\rangle_{c'}|H\rangle_{t_1'}|V\rangle_{t_3'}\\&+a_3|H\rangle_{c'}|V\rangle_{t_1'}|H\rangle_{t_3'}+a_4|H\rangle_{c'}|V\rangle_{t_1'}|V\rangle_{t_3'}\\&+a_5|V\rangle_{c'}|H\rangle_{t_1'}|H\rangle_{t_3'}+a_6|V\rangle_{c'}|V\rangle_{t_1'}|H\rangle_{t_3'}\\&+a_7|V\rangle_{c'}|H\rangle_{t_1'}|V\rangle_{t_3'}+a_8|V\rangle_{c'}|V\rangle_{t_1'}|V\rangle_{t_3'}\\&+a_1|H\rangle_{c'}|H\rangle_{t_1'}|H\rangle_{t_4'}+a_2|H\rangle_{c'}|H\rangle_{t_1'}|V\rangle_{t_4'}\\&+a_3|H\rangle_{c'}|V\rangle_{t_1'}|H\rangle_{t_4'}+a_4|H\rangle_{c'}|V\rangle_{t_1'}|V\rangle_{t_4'}\\&-a_5|V\rangle_{c'}|H\rangle_{t_1'}|H\rangle_{t_4'}-a_6|V\rangle_{c'}|V\rangle_{t_1'}|H\rangle_{t_4'}\\&-a_7|V\rangle_{c'}|H\rangle_{t_1'}|V\rangle_{t_4'}-a_8|V\rangle_{c'}|V\rangle_{t_1'}|V\rangle_{t_4'}\\&+a_1|H\rangle_{c'}|H\rangle_{t_2'}|H\rangle_{t_3'}+a_2|H\rangle_{c'}|H\rangle_{t_2'}|V\rangle_{t_3'}\\&+a_3|H\rangle_{c'}|V\rangle_{t_2'}|H\rangle_{t_3'}+a_4|H\rangle_{c'}|V\rangle_{t_2'}|V\rangle_{t_3'}\\&-a_5|V\rangle_{c'}|H\rangle_{t_2'}|H\rangle_{t_3'}-a_6|V\rangle_{c'}|V\rangle_{t_2'}|H\rangle_{t_3'}\\&-a_7|V\rangle_{c'}|H\rangle_{t_2'}|V\rangle_{t_3'}-a_8|V\rangle_{c'}|V\rangle_{t_2'}|V\rangle_{t_3'}\\&+a_1|H\rangle_{c'}|H\rangle_{t_2'}|H\rangle_{t_4'}+a_2|H\rangle_{c'}|H\rangle_{t_2'}|V\rangle_{t_4'}\\&+a_3|H\rangle_{c'}|V\rangle_{t_2'}|H\rangle_{t_4'}+a_4|H\rangle_{c'}|V\rangle_{t_2'}|V\rangle_{t_4'}\\&+a_5|V\rangle_{c'}|H\rangle_{t_2'}|H\rangle_{t_4'}+a_6|V\rangle_{c'}|V\rangle_{t_2'}|H\rangle_{t_4'}\\&+a_7|V\rangle_{c'}|H\rangle_{t_2'}|V\rangle_{t_4'}+a_8|V\rangle_{c'}|V\rangle_{t_2'}|V\rangle_{t_4'}].\end{aligned}\quad(19)$$

The Fredkin gate is achieved after the target photons pass through paths t_1' and t_3', or equally pass through paths t_2' and t_4'. For other outcomes of QND detectors, that is, the target photons pass through paths t_1' (t_2') and t_4' (t_3'), the Fredkin gate can be implemented by a σ_z operation on path c'.

If other phases are introduced by homodyne measurement, we can also gain the similar state given by Eq. (18) by utilizing the U operation according to the outcome of homodyne measurement through a classical feedforward. The correspondence between phase shifts in the coherent state and the U operations performed on the two target photons is shown in Table 1. Using the similar method in the case of no phase shift, we can implement the Fredkin gate by σ_z operations on corresponding paths according to the outcomes of the QND detectors. The error probability of the gate is $P_{\text{error}} = P_{\text{error}_1} + P_{\text{error}_2} + P_{\text{error}_3}$, where $P_{\text{error}_j} = (1/2)\text{erfc}[X_{\text{d}_j}/2\sqrt{2}]$ is the error probability induced by the overlap between the two Gaussian curves $f(X, \alpha\cos\beta_{j-1})$ and $f(X, \alpha\cos\beta_j)$ ($\beta_j = j\theta$). We have $P_{\text{error}} < 10^{-5}$ when $\alpha\theta^2 > 9$, so the success probability of our scheme for the Fredkin gate is almost unitary, and no auxiliary photons are required.

If the swap gate in the Fredkin gate is replaced by a CNOT gate or other arbitrary two-qubit unitary gate, it is sufficient to realize the Toffoli gate or the controlled-U gate. For the Toffoli gate, we can use the CNOT gate mentioned in previous section, so the success probability for this Toffoli gate is also nearly 100%. While the success probability for the controlled-U gate is determined by the probability of the arbitrary unitary gate. Obviously, even with the same probability for the unitary gate, the success probability for the controlled gates in our scheme are much higher than that in Ref. [20]. Those gates can also be implemented nonlocally with the method mentioned in the previous section.

Table 1. Correspondence between the phase shift in the coherent state and the U operation performed on the two target photons.

The phase shift in $\|\alpha\rangle$	U operation
0	$I_3 \otimes I_5 \otimes U_{46}^{\text{SWAP}}$
$\pm\theta$	$I_3 \otimes I_6 \otimes U_{45}^{\text{SWAP}}$
$\pm 2\theta$	$I_4 \otimes I_5 \otimes U_{36}^{\text{SWAP}}$
$\pm 3\theta$	$I_4 \otimes I_6 \otimes U_{35}^{\text{SWAP}}$

4. Discussion and conclusion

Our schemes are based on cross-Kerr nonlinearity and the homodyne detection of the phase shifts of the coherent states. However, the cross-Kerr effect is still a big challenge experimentally. The natural cross-Kerr nonlinearities are extremely weak,[22] and Kerr phase shift is only $\tau \approx 10^{-18}$ when operating in the optical single-photon system.[23] Hence, it is difficult to determine the phase shift of the coherent state due to the impossible discrimination of two overlapping coherent states, which will decrease the success probability of the present schemes. Fortunately, much progress has been made in Kerr nonlinearity and homodyne detection.[24,27] In 2003, Hofmann *et al.* showed that the maximal nonlinear π phase shift can be obtained with a single two-level atom in a one-sided cavity,[24] and it is possible to use resonant light to obtain a nonlinearity that is sensitive to individual excitations of the atom. It is worth noting that nearly deterministic discrimination for the phase shift of the coherent state is possible only if the requirement $\alpha\theta^2 \gg 1$ is satisfied.[15] This means that we can experimentally realize the weak cross-Kerr nonlinearity ($\theta \ll 1$) as long as the amplitude of the probe beam is sufficiently large, which is potentially available experimentally. For the experimental realization of our scheme, we can use Kerr mediums with a different coupling property, or control the interaction time with the same Kerr medium to realize the different phase shifts introduced in this paper. Moreover, it is significant to realize these phase shifts with smaller cross-Kerr nonlinearity. Wang *et al.* employed an optical device based on a high-quality ring cavity constructed by both two BSs and mirrors, and fed by a coherent state.[25] Such a device can substantially amplify the nonlinearity effect, which makes it possible to realize different phase shifts with tiny cross-Kerr nonlinearity. There are other techniques to realize our scheme, for

example, the double cross-phase modulation technique used in Ref. [26], and the displacement-controlled photon-number-resolving (PNR) detector used in Ref. [27]. That is to say, if we can choose appropriate Kerr media and effective measurement of the phase shift of the coherent beam, then weak cross-Kerr nonlinearity can be achieved efficiently, which makes our schemes more feasible. The QND detectors are indispensable for judging which paths the signal photons pass through, and a corresponding classical feedforward will be performed according to their outcomes. As a potential selection, the classical switch can be used to combine two target output ports to one port. However, it is not easy to implement with the present techniques.

In this paper, schemes for two-qubit and three-qubit controlled gates are proposed, utilizing the weak cross-Kerr nonlinearity. These schemes are almost deterministic due to the application of the cross-Kerr nonlinearity and QND detectors, and require no ancilla photon. For the two-qubit controlled-Z gate, we use beam splitters to modulate the phase of the two-photon state. To make the three-qubit Fredkin gate deterministic, we implement the U operations according to the outcomes of homodyne measurement through a classical feedforward. The fewer resources required and the higher success probability of these gates make our scheme feasible with current technology, and useful for universal quantum communication and quantum computation.

References

[1] Spiller T P, Munro W J, Barrett S D and Kok P 2005 *Contemp. Phys.* **46** 407

[2] Tang S Q, Zhang D Y, Wang X W, Xie L J and Gao F 2011 *Chin. Phys. B* **20** 040308

[3] Zhong W X, Cheng G L and Chen A X 2010 *Chin. Phys. B* **19** 110501

[4] Shi H M, Yu Y F and Zhang Z M 2012 *Chin. Phys. B* **21** 064205

[5] Knill E, Laflamme R and Milburn G J 2001 *Nature* **409** 46

[6] Pittman T B, Jacobs B C and Franson J D 2001 *Phys. Rev. A* **64** 062311

[7] Pittman T B, Jacobs B C and Franson J D 2002 *Phys. Rev. Lett.* **88** 257902

[8] Bao X H, Chen T Y, Zhang Q, Yang J, Zhang H, Yang T and Pan J W 2007 *Phys. Rev. Lett.* **98** 170502

[9] Hofmann H F and Takeuchi S 2002 *Phys. Rev. A* **66** 024308

[10] Kiesel N, Schmid C, Weber U, Ursin R and Weinfurter H 2005 *Phys. Rev. Lett.* **95** 210505

[11] Wang H F, Shao X Q, Zhao Y F, Zhang S and Hwang K 2010 *J. Opt. Soc. Am. B* **27** 27

[12] Cao S and Fang M F 2006 *Chin. Phys.* **15** 276

[13] Gong Y X, Guo G C and Ralph T C 2008 *Phys. Rev. A* **78** 012305

[14] Barrett S D, Kok P, Nemoto K, Beausoleil R G, Munro W J and Spiller T P 2005 *Phys. Rev. A* **71** 060302

[15] Nemoto K and Munro W J 2004 *Phys. Rev. Lett.* **93** 250502

[16] Guo Q, Bai J, Cheng L Y, Shao X Q, Wang H F and Zhang S 2011 *Phys. Rev. A* **83** 054303

[17] Kok P 2008 *Phys. Rev. A* **77** 013808

[18] Xia Y, Song J, Lu P M and Song H S 2011 *J. Phys. B* **44** 025503

[19] Xiu X M, Dong L, Gao Y J and Yi X X 2012 *Quantum Inf. Comput.* **12** 0159

[20] Lin Q and Li J 2009 *Phys. Rev. A* **79** 022301

[21] Munro W J, Nemoto K, Spiller T P, Barrett S D, Kok P and Beausoleil R G 2005 *J. Opt. B: Quantum Semiclass. Opt.* **7** S135

[22] Kok P, Munro W J, Nemoto K, Ralph T C, Dowing J P and Milburn G J 2007 *Rev. Mod. Phys.* **79** 135

[23] Kok P, Lee H and Dowling J P 2002 *Phys. Rev. A* **66** 063814

[24] Hofmann H F, Kojima K, Takeuchi S and Sasaki K 2003 *J. Opt. B* **5** 218

[25] Wang X W, Zhang D Y, Tang S Q, Xie L J, Wang Z Y and Kuang L M 2012 *Phys. Rev. A* **85** 052326

[26] He B, Ren Y H and Bergou J A 2009 *Phys. Rev. A* **79** 052323

[27] Wittmann C, Andersen U L, Takeoka M, Sych D and Leuchs G 2010 *Phys. Rev. A* **81** 062338